J Appl Physiol 102: 2315–2323, 2007.
First published March 8, 2007; doi:10.1152/japplphysiol.00856.2006.

Quantitative assessments of morphological and functional properties of biological trees based on their fractal nature

Akira Kamiya[1] and Tatsuhisa Takahashi[2]

[1]Nihon University General Research Center, Tokyo; and [2]Department of Mathematical Information Science, Asahikawa Medical College, Asahikawa, Japan

Submitted 3 August 2006; accepted in final form 2 March 2007

Kamiya A, Takahashi T. Quantitative assessments of morphological and functional properties of biological trees based on their fractal nature. *J Appl Physiol* 102: 2315–2323, 2007. First published March 8, 2007; doi:10.1152/japplphysiol.00856.2006.—The branching systems in our body (vascular and bronchial trees) and those in the environment (plant trees and river systems) are characterized by a fractal nature: the self-similarity in the bifurcation pattern. They increase their branch density toward terminals according to a power function with the exponent called fractal dimension (D). From a stochastic model based-on this feature, we formulated the fractal-based integrals to calculate such morphological parameters as aggregated branch length, surface area, and content volume for any given range of radius (r). It was followed by the derivation of branch number and cross-sectional area, by virtue of the logarithmic sectioning of the r axis and of the branch radius-length relation also given by a power function of r with an exponent (α). These derivatives allowed us to quantify various hydrodynamic parameters of vascular and bronchial trees as fluid conduit systems, including the individual branch flow rate, mean flow velocity, wall shear rate and stress, internal pressure, and circumferential tension. The validity of these expressions was verified by comparing the outcomes with actual data measured in vivo in the vascular beds. From additional analyses of the terminal branch number, we found a simple equation relating the exponent (m) of the empirical power law (Murray's so-called cube law) to the other exponents as ($m = D + \alpha$). Finally, allometric studies of mammalian vascular trees revealed uniform and scale-independent distributions of terminal arterioles in organs, which afforded an infarct index, reflecting the severity of tissue damage following arterial infarction.

fractal dimension; allometric scaling; Murray; vascular beds; wall shear stress

AS MANDELBROT (24) stated in his elegant monograph, biological branching systems such as vascular, bronchial, and plant trees all exhibit fractal nature, i.e., a scale-independent self-similarity in the bifurcation pattern of their architecture (2, 10). The fractal dimensions (D) of these biological systems have been measured using various techniques, as reported in the literature for vascular (5, 27, 39), bronchial (21, 31), and plant (26, 28, 40) trees. In all but a few cases (27, 28), the entire branch distribution is well simulated by a power function with a single exponent ($-D$), as discussed later. The arguments developed in these investigations have tended to concentrate on profound mathematical implications underlying the fractal geometry (2, 24); however, its applicability to practical problems in biology has been less explored. Here, we try to supplement some pragmatic methodology to use these D values in quantitative analyses of the biological branching systems, which may shed light on additional significance of the fractal theory in biological sciences.

The primary aim of this study is to show that the fundamental quantities of the fractal branching systems can be formulated in simple rational functions. On the basis of a stochastic model linking the probability of branch density with aggregated branch length, morphological parameters are expressed in plain definite integrals with D for a desired range of branch radius. Then, fluid dynamic parameters of vascular and bronchial trees as the conduit systems are derived in power functions of radius including D in the exponents. The reliability of these expressions will be examined by comparing their outcomes with actual data measured in vivo in the vascular beds (47).

Another aim of this study is to clarify the relationship between the fractal dimension and the exponent of the empirical power law in the vascular and bronchial trees (Murray's so-called cube law), of which close correlation has been delineated by Mandelbrot (24). We will present a patent mathematical equation relating these two parameters, in corporation with the branch length-radius relationship by Suwa and Takahashi (41).

Further discussion will be extended for applicability of the present fractal models to various biological problems. This included the allometric assessment of the terminal branch number of the vascular tree in mammalian organs, which gave us the opportunity to propose an infarct index, a quotient of clinical significance.

METHODS

The basic model in this study is constructed on the common stochastic characteristics of fractal trees. Its principle, however, is best interpreted by considering a situation measuring a fractal dimension (D) of an in situ vascular tree from cross sections of the host tissue specimen stained with a blood vessel marker (5, 21; Fig. 1*A*). Any cross section is randomly selected and is examined microscopically by altering the resolution suitable to relevant vascular sizes. The radius of each vessel is measured from the minor axis of its elliptic cut end (Fig. 1*B*), and the number of vessels larger in radius than the variable (r) is counted to calculate the density per unit area. The density data accumulated by repeating this procedure for other sections are used to determine the dimension D from the negative slope of their log-log plot against r (Fig. 1*C*). The above procedure to determine D is similar to that of the ordinary box-counting method (26, 27). The estimated value of D must be between one and two, because data are sampled from planes (24). When the acquired power function of r is normalized with the total count, it represents the probability $\Phi(r)$ that a branch larger than r in radius is observed in any unit area of a cross

Address for reprint requests and other correspondence: T. Takahashi, Dept. of Math. Info. Sci., Asahikawa Medical College, Asahikawa 078-8510, Japan (e-mail: ryushow@asahikawa-med.ac.jp).

The costs of publication of this article were defrayed in part by the payment of page charges. The article must therefore be hereby marked "*advertisement*" in accordance with 18 U.S.C. Section 1734 solely to indicate this fact.

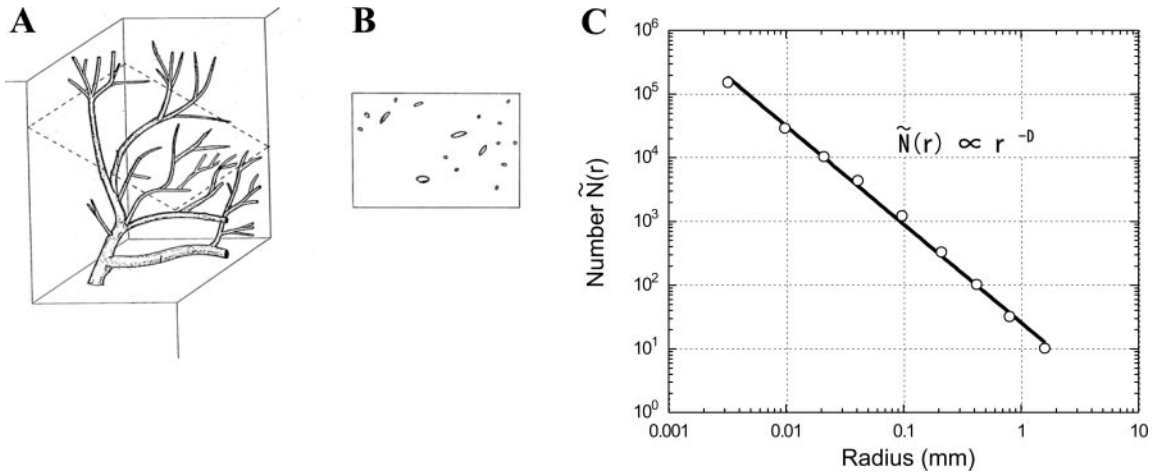

Fig. 1. Schematic illustrations for interpreting the method to measure a fractal dimension (D) of a natural branching system. *A:* in situ vascular tree in the tissue specimen. *B:* cross section of the tissue including the elliptic cut ends of vascular branches of various sizes, the short axes of which designate the vessel radii. *C:* when the number of branches [$\tilde{N}(r)$] larger in radius than the variable (r) is counted and plotted against r on a log-log scale, the gradient of the linear slope represents the dimension D of the fractal tree. Data points in *C* are plotted by partly modifying the data measured in the rat brain vasculature by Matsuo et al. (27; with permission).

section and can be written with the probability density function $\varphi(r)$ as follows:

$$\Phi(r) = \int_r^\infty \varphi(r)dr, \quad \varphi(r) = \kappa r^{-D-1}, \quad \kappa = \frac{D}{r_t^{-D} - r_o^{-D}}, \qquad (1)$$

The coefficient κ is given as above, because in biological trees, the minimum branch radius at the terminals (r_t) is known to be almost uniform (37) and its value as well as the maximum radius at the origin (r_o) is usually measurable [$\varphi(r) = 0$, for $r < r_t$ or $r > r_o$ and $\int_0^\infty \varphi(r)dr = \int_{r_t}^{r_o} \varphi(r)dr = 1$]. We will discuss later about the morphological and functional uniformity of the terminal branches in these trees.

A novel point in the present stochastic approach is to introduce a new term, "aggregated branch length," and to relate it to the above probability density function $\varphi(r)$ under the stationary condition. The aggregated branch length is defined as the sum of the branch length of vessels in a group sorted for radius around r within a certain minute deviation (dr). Obviously, the longer the aggregated branch length in the host specimen is, the more frequently the vessels in the group are observed in any cross section. This linear relationship is simply expressed by employing the density function of the aggregated length $l_a(r)$ as follows:

$$l_a(r)dr = \lambda\varphi(r)dr, \qquad (2)$$

where λ is a scale factor in the length dimension. From *Eqs. 1* and *2,* the aggregated branch length (ΔL) within a certain radius range $r_1 \leqq r \leqq r_2$ is calculated by integrating $l_a(r)dr$ over the range:

$$\Delta L = \int_{r_1}^{r_2} l_a(r)dr = \frac{\lambda\kappa}{-D}(r_2^{-D} - r_1^{-D}). \qquad (3)$$

It is evident that the coefficient λ represents the entire branch length [$\lambda = \int_{r_1}^{r_2} l_a(r)dr$]. Analogously, the surface area (ΔS) and content volume (ΔV) of the branches are obtained by integrating $2\pi r l_a(r)dr$ and $\pi r^2 l_a(r)dr$ for the given radius range:

$$\Delta S = \int_{r_1}^{r_2} 2\pi r l_a(r)dr = \frac{2\pi\lambda\kappa}{-D+1}(r_2^{-D+1} - r_1^{-D+1}), \qquad (4)$$

$$\Delta V = \int_{r_1}^{r_2} \pi r^2 l_a(r)dr = \frac{\pi\lambda\kappa}{-D+2}(r_2^{-D+2} - r_1^{-D+2}). \qquad (5)$$

These fractal-based integrals are probably the first mathematical formulations that clearly describe the structural parameters of the trees with discrete functions of branch radii. Notice that the distributions of these morphological quantities along the vessel size have conventionally been estimated only in semi-quantitative ways in the systemic vasculatures (6, 36) or calculated in the symmetric and regularly downsizing branch models as a function of branch generation in the pulmonary arterial and bronchial systems (3, 23, 44).

By introducing several basic assumptions, the above integrals allow us to quantify the functional parameters of vascular and bronchial trees as fluid conduit systems, in combination with the branch length-radius (L_b-r) relationship established by Suwa and Takahashi (41):

$$L_b(r) = \beta r^\alpha. \qquad (6)$$

The values of the exponent (α) in various vascular beds are clustered around 1.0 (41). A similar relation has been reported for the bronchial system (43) as well as plant trees (32).

The first assumption employed is the steady state of fluid-dynamic parameters under constant flow distribution of incompressible fluid. If pulsations of the branch radius and flow due to cardiac beats or pulmonary ventilation are significant, their mean values through the cycles are used for calculations of the parameters. Otherwise, more elaborate models including pulsatile variables [*e.g.,* Painter et al. (33)] should be employed. It is also assumed that in the vascular tree, all vessels except capillaries are fully recruited.

The derivation of the functional parameters is initiated by evaluating the branch number $N_b(r)$ as a discrete function of radius r. To do so, we derive the expectation of aggregated branch length $\bar{L}_a(r)$ at r from the integral in *Eq. 3,* according to the logarithmic sectioning of the r axis (see APPENDIX A):

$$\bar{L}_a(r) = \lambda\kappa r^{-D}.$$

Then, the branch number $N_b(r)$ is acquired from the ratio $\bar{L}_a(r)/L_b(r)$:

$$N_b(r) = \frac{\bar{L}_a(r)}{L_b(r)} = \frac{\lambda\kappa}{\beta} r^{-D-\alpha} = \left(\frac{r}{r_o}\right)^{-D-\alpha}, \qquad (7)$$

since the number at the origin is unity [$N_b(r_o) = 1$, then $\lambda\kappa/\beta = r_o^{D+\alpha}$].

The above expression of $N_b(r)$ allows similar fractal-based formulations for cross-sectional area (A_c), mean flow velocity (U_m), individual branch flow (F_b), and wall shear rate ($\dot{\gamma}_w$), all in the forms of the ratio, r/r_o or r/r_t, with their values at the origin (A_{co}, U_{mo}, F_{bo}, and $\dot{\gamma}_{wo}$) or at the terminals (A_{ct}, U_{mt}, F_{bt}, and $\dot{\gamma}_{wt}$):

$$A_c(r) = \pi r^2 N_b(r) = A_{co}\left(\frac{r}{r_o}\right)^{-D-\alpha+2} = A_{ct}\left(\frac{r}{r_t}\right)^{-D-\alpha+2},$$
$$U_m(r) = \frac{F_{bo}}{A_c(r)} = U_{mo}\left(\frac{r}{r_o}\right)^{D+\alpha-2} = U_{mt}\left(\frac{r}{r_t}\right)^{D+\alpha-2}, \quad (8)$$
$$F_b(r) = \pi r^2 U_m(r) = F_{bo}\left(\frac{r}{r_o}\right)^{D+\alpha} = F_{bt}\left(\frac{r}{r_t}\right)^{D+\alpha},$$
$$\dot{\gamma}_w(r) = \frac{4U_m(r)}{r} = \dot{\gamma}_{wo}\left(\frac{r}{r_o}\right)^{D+\alpha-3} = \dot{\gamma}_{wt}\left(\frac{r}{r_t}\right)^{D+\alpha-3}.$$

Since $N_b(r)$ in *Eq. 7* implies the expectation of the branch number, the derived parameters in *Eq. 8* represent the averaged values for the same size branches, which absorb the statistical deviations due to the asymmetric dichotomy involvement (23) and so on (see APPENDIX B).

The profile of the internal pressure $P(r)$ is another important variable of fluid dynamics in the conduit systems, particularly in the vascular system. Hagen-Poiseuille's law indicates that the pressure drop (ΔP) against flow F_b along a branch of radius r and length L_b is written as:

$$\Delta P = \frac{8\mu(r)F_b}{\pi r^4}L_b \approx \frac{8\mu(r)U_m(r)}{r^2}L_b,$$

where $\mu(r)$ is the radius-dependent fluid viscosity and $U_m(r)$ is the mean flow velocity in *Eq. 8.* Because the differentiation of *Eq. 6* with respect to r yields $dL_b/dr = \beta\alpha r^{\alpha-1}$ and $\Delta P/L_b = \partial P/\partial L_b$, the pressure gradient against radius (dP/dr) is written as:

$$\frac{dP}{dr} = \frac{dL_b}{dr}\frac{\partial P}{\partial L_b} \approx 8\beta\alpha r^{\alpha-3}\mu(r)U_m(r).$$

When we deal with blood viscosity in the vascular system, the simplest mathematical model of its vessel-radius dependency $\mu(r)$ has been proposed by Haynes (11):

$$\mu(r) = \frac{\mu_\infty}{(1+\delta/r)^2}. \quad (9)$$

As seen in Fig. 2, this equation well simulates the apparent viscosity data of blood at least for the vessel sizes relevant in this study ($r \geq 4$ μm), if appropriate values are assigned to the saturated viscosity at a large tube (μ_∞) and to the constant of red cell size order (δ). Accordingly, the pressure gradient in the vascular system against branch radius, dP/dr, can be expressed in the following equation:

$$\frac{dP}{dr} \approx \pm k\frac{r^{D+2\alpha-3}}{(r+\delta)^2}, \quad k = \frac{8\alpha\beta^2\mu_\infty F_{bo}}{\pi\lambda\kappa} \quad (10)$$

The symbol "±" corresponds to the arterial and venous sides, respectively. The pressure profile $P(r)$ is obtained by integrating the above differential equation. In general, the solution is given by binomial integration (42). However, in a special case where the exponent of r is equal to unity ($D + 2\alpha - 3 = 1$) and the terminal pressure (P_t) is constant as usual (37), $P(r)$ is written as:

$$P(r) \approx P_t \pm k\left[ln\left(\frac{r+\delta}{r_t+\delta}\right) + \delta\left(\frac{1}{r+\delta} - \frac{1}{P_t+\delta}\right)\right]. \quad (11)$$

It is also suggested in *Eq. 11* that when the constant k in *Eq. 10* is difficult to determine and the pressure at the origin (P_o) is known, an alternative expression of $\pm k$ is useful:

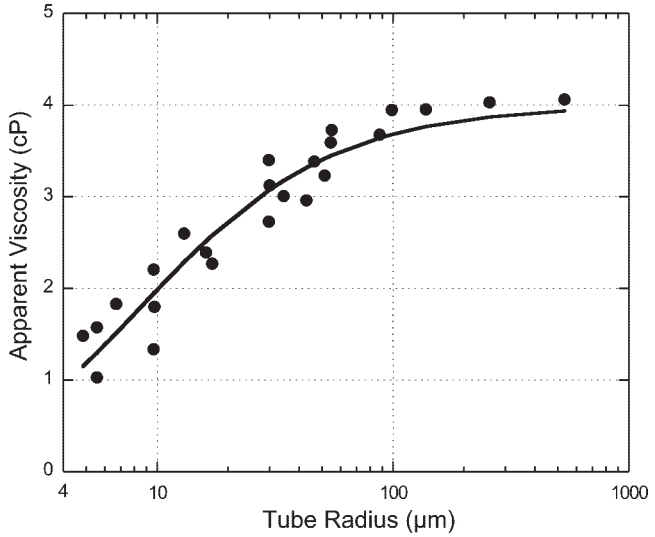

Fig. 2. Apparent blood viscosity data showing the tube radius dependency and its simulation curve proposed by Haynes (11). ●, Viscosity data of human blood measured in vitro with tubes of various radii, and the solid line shows the simulation curve in *Eq. 9* with the parameter values of μ_∞ = 4.0 cP and δ = 4.29 μm, which was determined by the least squares fitting to the data points (4).

$$\pm k = \frac{P_o - P_t}{\ln\left(\frac{r_o+\delta}{r_t+\delta}\right) + \delta\left(\frac{1}{r_o+\delta} - \frac{1}{r_t+\delta}\right)}.$$

Note that the term ($P_o - P_t$) is negative in the venous system.

The following analyses are concerned with the relation of the present fractal model to the empirical power law, which is well known to hold for the bifurcating structure in vascular and other biological trees. At every branching point, the radius of a mother branch (r_0) is related to those of daughter branches (r_1 and r_2) by a certain number (m) with a small deviation (19):

$$r_0^m = r_1^m + r_2^m. \quad (12)$$

Mandelbrot (24) called this number "m" as the diameter exponent (by designating it with a symbol "Δ") and ascribed it to the proof that the biological trees are possessed of a fractal nature, i.e., self-similarity in the branching pattern. The system-specific values of m, estimated morphometrically in various mammal vascular beds, range from 2.7 to 3.0 (15, 16, 20, 29, 35, 41), whereas those in the bronchial and plant trees are reported to be around 3.0 (14, 21, 22, 23) and 2.5 (30), respectively.

In order to clarify the relationship between the fractal dimension D and the diameter exponent m, let us consider a set of three trees, the origin of which is shared by the mother and daughter branches, as shown in Fig. 3. Obviously, the number of terminal branches of the mother tree is equal to the sum of those of the daughter trees. When the terminal radii r_t are largely equal in these trees as ordinal, this relationship is written by applying the terminal branch number $N_b(r_t)$ in *Eq. 7* as follows:

$$\left(\frac{r_t}{r_0}\right)^{-(D+\alpha)} = \left(\frac{r_t}{r_1}\right)^{-(D+\alpha)} = \left(\frac{r_t}{r_2}\right)^{-(D+\alpha)} \quad or \quad r_0^{D+\alpha} = r_1^{D+\alpha} + r_2^{D+\alpha}.$$

In comparison with *Eq. 12,* we have a new formula,

$$m = D + \alpha. \quad (13)$$

This quite simple equation directly links the empirical power law and the present fractal model of the biological branching systems.

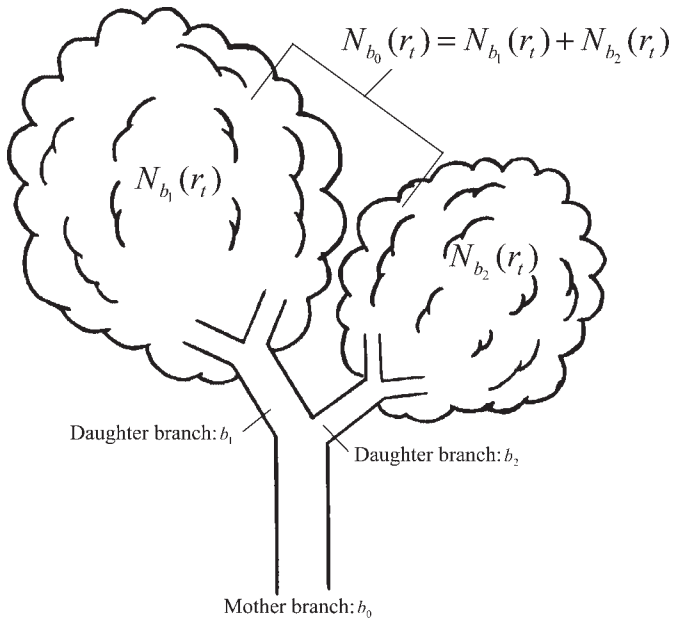

Fig. 3. Schematic drawing interpreting a very simple relationship of terminal branch numbers in any tree, indicating that when a mother branch (b_0) is divided into 2 daughter branches (b_1 and b_2), the terminal number of the b_0 tree [N_{b0} (r_t)] is equal to the sum of the individual terminal numbers of trees b_1 and b_2 [N_{b1} (r_t) + N_{b2} (r_t)].

RESULTS

When the values of D and λ are given, the aggregated branch length ΔL, surface area ΔS, and content volume ΔV can be calculated from the fractal-based integrals in *Eqs. 3* to *5* for any radius range. Figure 4*A* illustrates an example of such calculations for three different values of D (= 1.4, 1.6, and 1.8), which were carried out for the systemic arterial system (ΔL_{SA}, ΔS_{SA}, and ΔV_{SA}) in an adult human (70 kg in body weight, W_b), by assessing λ from the physiological estimate of total systemic arterial volume (700 ml, 6). The relative distributions of these morphological parameters to the totals within logarithmically scaled radius ranges are also illustrated in Fig. 4*B*. Note the different trends in these relative distributions, markedly increasing in ΔL_{SA}, but decreasing in ΔV_{SA} toward the terminals. Such tendencies clearly differing in the distributions of the individual morphological parameters over the entire radius range have not been well explored in conventional studies, at least in the systemic vasculatures (6, 36).

Concerning the functional parameters, the reliability of the formulae in *Eqs. 8–11* was examined by comparing their outcomes with actual measurements obtained in the vascular system. Figure 5 illustrates in vivo data of mean red cell flow velocity and blood pressure, measured in the peripheral vascular beds of the rat mesentery by Zweifach and Lipowsky (47), probably under considerably vasodilated conditions. These data are quite rare and valuable because they are plotted against vessel radius at each measuring site. The thin broken lines indicate the curves of mean flow velocity $U_m(r)$ calculated from *Eq. 8* for $D = 1.75 \pm 0.05$ and the value of $\alpha = 1.13$ reported for this vascular bed (41). As seen in Fig. 5, the obtained curves for $D = 1.75$ well simulated the actual data of mean flow velocity on both the arterial and venous sides. In addition, the exponent of r in *Eq. 10* according to D (=1.75) and α (=1.13) above, happened to be very close to 1.0 ($D + 2\alpha - 3 = 1.01$). Therefore, the pressure profiles were simulated using *Eq. 11* as designated by the broad solid lines in Fig. 5. The curves showed fine fitting to the in vivo pressure data in both the arterial and venous vascular beds. Such agreements between the in vivo data and the simulated curves in Fig. 5 confirmed the reliability of the proposed fractal model in quantitative assessments of hemodynamic parameters in the systemic circulation.

From $\dot{\gamma}_w(r)$, $\mu(r)$, and $P(r)$ in *Eqs. 8, 9,* and *11,* we are able to calculate wall shear stress [$\tau_w(r) = \mu(r)\dot{\gamma}_w(r)$] and circumferential wall tension [$T_c(r) = rP(r)$], two major biomechanical factors that induce the adaptive remodeling of vascular walls (17, 25). Figure 6 depicts the distributions of these factors in the vascular system, computed over the entire range of vessel radius (4 μm $\sim$ 1 cm) using the values of $D = 1.75 \pm 0.05$, the same value of α and other coefficients as those in Fig. 5. The profiles of $\tau_w(r)$ visualized by the three curves to the individual D values revealed convex curves. They attained their peaks in a radius range from 30 to 90 μm, although the shear stress levels were rather higher compared with conventional data (15), probably due to considerably high flow velocity data in Fig. 5 (47). On the other hand, the profile of $T_c(r)$ was presented by a single curve, because the exponents of r in *Eq. 10* ($D + 2\alpha - 3 = 0.96$, 1.01, and 1.06) corresponding to the above D values were all close to 1.0 and *Eq. 11* could be employed for $P(r)$ calculation. The curve of $T_c(r)$ showed a largely monotonous decline toward the terminals in both sides, except for the portion of very large veins.

Regarding the relation between the power law exponent and the fractal dimension in *Eq. 13* ($m = D + \alpha$), the values of $D = 1.75$ and $\alpha = 1.13$ in Fig. 5 rendered $m = 2.88$, which fell just within the range of conventional m estimates of 2.7 $\sim$ 3.0 for the vascular trees (15, 16, 20, 29, 35, 41).

DISCUSSION

The arguments so far have been carried out under the assumption that any branching system is entirely prescribed by a single fractal dimension. A few studies (27, 28), however, have shown that it is not true in some cases, where the system appears to be ruled by two different dimensions for large and small radius ranges. It is, however, not a serious problem for the proposed fractal model, being essentially based on definite integrals, to rewrite the model using multiple D values, so long as the radius zones corresponding to them are explicitly defined. A model of double diameter exponents ($m = 2$ and 3) in the vascular tree was also adopted by West et al. (45) for analyses of the allometric scaling law in mammals. In addition, several studies (33, 45) proposed dynamic models, in which pulsatile movement of the duct wall is involved with pressure and flow variations due to cardiac beats or pulmonary ventilation, although the model in this study is confined to the steady-flow condition.

The other major assumption underlying this study is the uniform size of terminal branches in biological trees. In comparative animal physiology (37, 38), it is well established that the terminal branches in the vascular and bronchial trees are body scale-independently uniform in their size. Moreover, we usually observe in plant trees that the terminal branches are formed in a species-specific uniform shape and size. The terminal

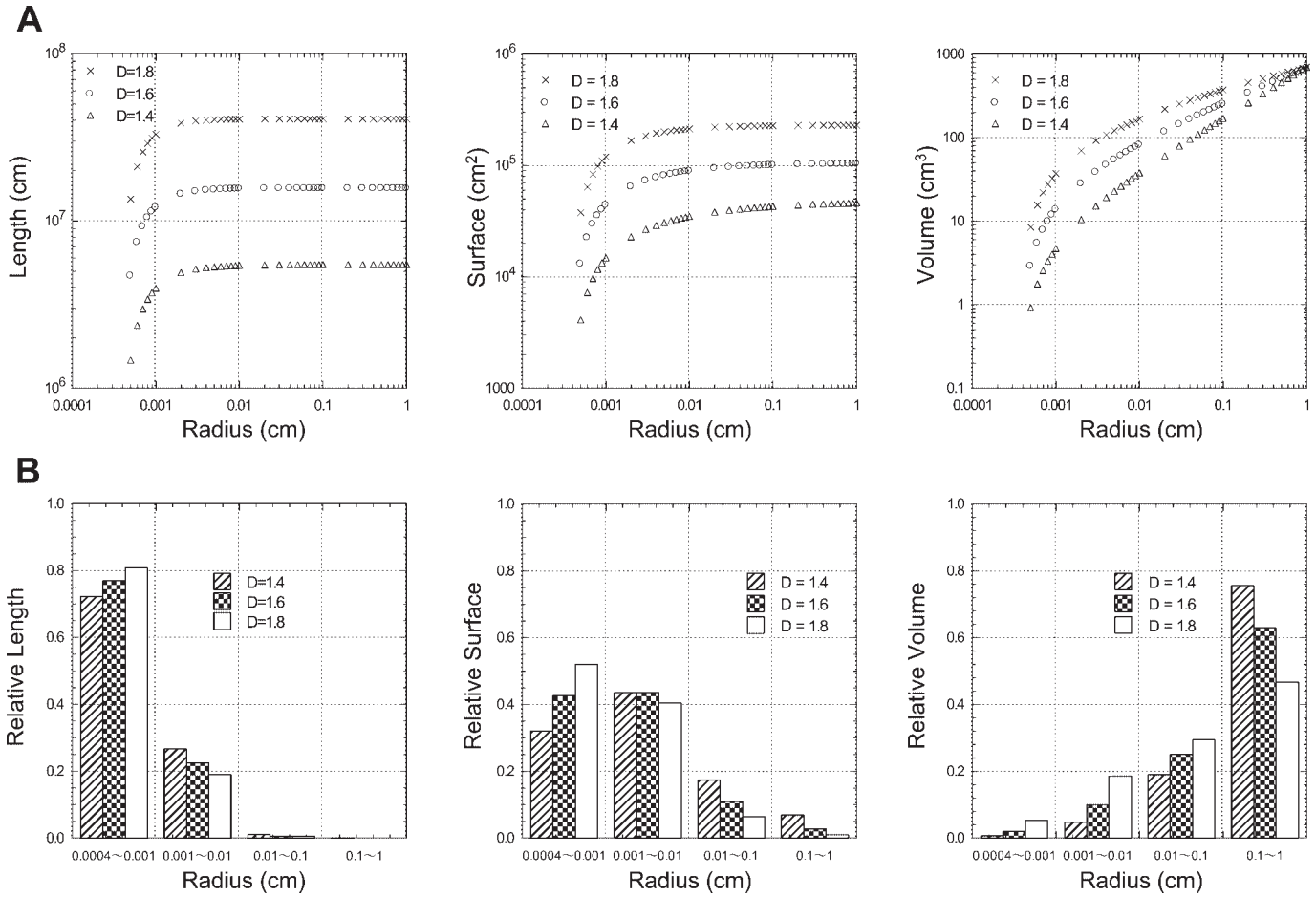

Fig. 4. Regional distributions of morphological parameters for the systemic arterial systems of a 70-kg human. *A:* log-log plots of aggregated branch length (ΔL_{SA}), surface area (ΔS_{SA}), and content volume (ΔV_{SA}) vs. branch radius (r) calculated from *Eqs. 3–5.* The parameters employed include: $D = 1.4$, 1.6, and 1.8; $r_1 = r_t = 4$ μm; $r_2 \leq r_o = 1$ cm; and total systemic arterial volume (= 700 ml, Ref. 6). *B:* relative values of ΔL_{SA}, ΔS_{SA}, and ΔV_{SA} to the total values within the given ranges of radius for the above 3 values of D.

blood pressure in mammals is also known to be regulated at a constant, because the hydrostatic capillary pressure is one of the essential factors to control fluid balance across the capillary wall (38).

The results in Figs. 4 and 5 demonstrated that the fractal-based integrals and their derivatives can be feasibly applied to the assessments of morphological and functional quantities of the vascular system, although the applicable situation is limited to the stationary state, under which neither physiological remodeling nor pathological deterioration is taking place. These attempts may be extended to the bronchial system and the pulmonary functions as well. Compared with the bronchial tree model by Horsfield et al. (13, 14) and others (9, 21, 22, 23), one of the characteristics of the proposed model is that the available morphological information is only coordinated with the branch radius and is free from branch generation numbering (see APPENDIX B). In some cases, such a feature of this model may serve more direct approaches to various physiological phenomena taking place in the bronchial ducts and alveoli. For example, the regional distribution of surface area ΔS in the bronchial tree given by *Eq. 4* may facilitate simulations of heat and vapor dissipation through the duct wall. The distribution of content air volume ΔV estimated from *Eq. 5* may also provide an accurate modeling of diffusion and ventilation processes of gases in the bronchial duct branches and alveoli.

The application of this fractal model to plant trees is also promising. The fractal-based integral of content volume ΔV in *Eq. 5* suggests that only a few data for a tree, such as the species-specific D and trunk size, are sufficient for predicting the volume of wood in a relevant range of timber sizes contained in the tree. This kind of assessment would certainly be beneficial in forest resource management and its efficient industrial utilization. The integral of surface area ΔS in *Eq. 4* is also informative when tree bark contains products of agricultural or pharmaceutical interest. Furthermore, it is useful to estimate the oxygen production rate of a tree or a forest, which is one of essential factors in ecological assessments, through the leaf surface area calculable from the number of terminal branches using *Eq. 7.* Similar analyses can be extended to plant roots, because the root system possesses a fractal nature in the branching structure (40). Mass assessment of fine plant roots in the ground may help quantify their water-holding capacity, which is an important factor in protecting against floods and landslides after heavy rains.

Because these fractal trees are widely distributed in nature, applicable fields of the proposed model (*Eqs. 3–13*) are ex-

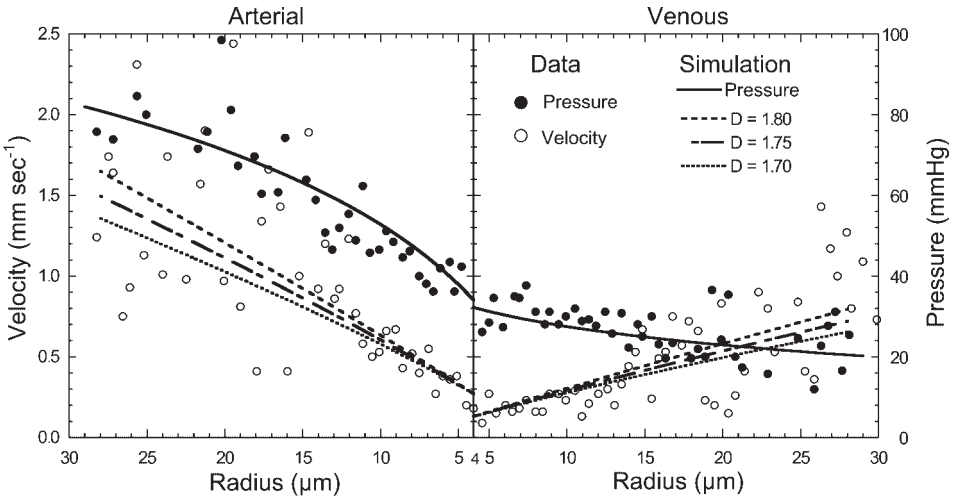

Fig. 5. In vivo data of mean red cell flow velocity (○) and of blood pressure (●) measured in the peripheral vascular beds of the rat mesentery (47) and their simulation curves of the fractal model. The thin broken lines indicate the mean flow velocity curves $U_m(r)$ calculated for $D = 1.75 \pm 0.05$ and $\alpha = 1.13$ (41) from *Eq. 8,* using the terminal velocity data ($U_{mt} = 0.27$ mm/s at the arteriolar end and $U_{mt} = 0.13$ mm/s at the venular end) sampled in this figure. The thick solid line indicates the pressure profile $P(r)$ calculated from *Eq. 11* using the data $\delta = 4.29$ μm and the sample data of $P_t = 34$ mmHg at $r_t = 4$ μm and $P_o = 82$ mmHg at $r_o = 29$ μm for the arterial side, and $P_t = 32$ mmHg at $r_t = 4$ μm and $P_o = 20$ mmHg at $r_o = 29$ μm for the venous side.

pected to be very vast, including cardiovascular and pulmonary physiology, pathology, and biomechanics, clinical medicine, botany, agriculture, forestry and related industrial technologies, ecology and environmental assessment, and many other areas. In addition to such pragmatic advantages, the proposed model may provide unique quantitative approaches to various biological problems, as described below.

The theoretical relationship between the empirical power law and the proposed fractal model in biological branching systems was clearly described by *Eq. 13* ($m = D + \alpha$) in this study. Mandelbrot (24) proclaimed their close correlation and called the diameter exponent "Δ" ($= m$) as a kind of fractal dimension. However, he referred no such relation as *Eq. 13,* probably because his concept of fractal dimension was too profound and comprehensive to encounter this kind of plain equality. Concise definition of D in the present stochastic model is essential to derive *Eq. 13,* with the aid of the branch length-radius relationship by Suwa and Takahashi (41). Anyway, a stable cross bridge has been established between the empirical power law and the fractal model in the branching systems. We are now able to convert any information of either side to the other.

In this study, the value of m was calculated from D (=1.75) and α (=1.13), yielding a figure "$m = 2.88$" that was well consistent with its conventional estimates as described before. In many cases, however, *Eq. 13* may be used to assess D, because the data of m for various tree systems have been accumulated among the arguments of the power law (14–16, 21–23, 29, 30, 35, 41) and many data of α are also available in the morphometric reports of the biological trees (32, 41, 43).

The reason why the diameter exponent m is close to 3 in the vascular system has been explained with the optimum model by Murray (29) that the cost function of a vessel branch, consisting of the mechanical energy expenditure due to viscous resistance and the chemical energy cost in proportion to blood volume, is minimized when $m = 3$ (the minimum work model). The physiological mechanism inducing this optimal relation was first experimentally confirmed by Kamiya and Togawa (17) to be the adaptive response of the vascular wall to fluid shear stress. The response was found to remodel the diameter so as to maintain the stress at a constant against flow changes and the diameter exponent m at 3. Many studies (15, 16, 20, 29, 35, 41), however, showed that the values of m reported for various vascular trees were slightly but always less than 3. A later survey by Kamiya et al. (15) also revealed a large difference in wall shear stress levels between the arterial and venous sides and vessel size dependency in both sides (see Fig. 6). These findings suggest a clear inconsistency

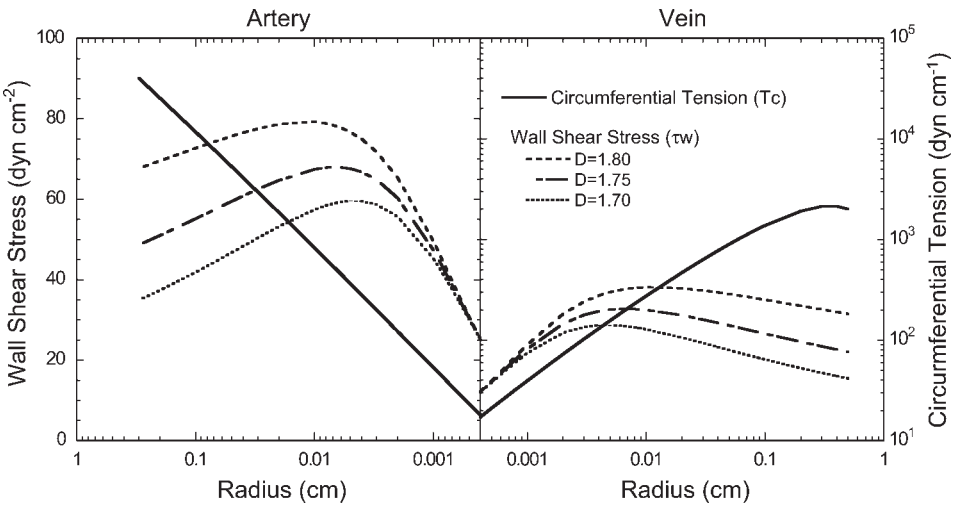

Fig. 6. Wall shear stress (τ_w) and circumferential wall tension (T_c) calculated for the entire range of the vascular radius 4 μm = $r_t \leq r \leq r_o = 1.0$ cm, by employing the same values of D ($=1.75 \pm 0.05$), α ($= 1.13$) and other coefficients as those in Fig. 5. The profile of τ_w (r) [$=\mu(r)\dot{\gamma}(r)$] is shown with 3 curves corresponding to the 3 values of D in either of the arterial and venous sides whereas that of T_c (r)[$=rP(r)$] is depicted with a single curve because $P(r)$ is calculated by *Eq. 11* (see text).

between the actual situations and the optimum state predicting even levels of the stress and the exponent anywhere in the vasculature. Although Karau et al. (19) ascribed this discrepancy to the heterogeneity of individual m values, another possible explanation is that some energy term, probably related to the circumferential tension or the internal pressure (34), might be lacking in the conventional cost function of the vascular system in the minimum work model (29). The profiles of wall shear stress (τ_w) and circumferential tension (T_c) depicted against branch radius in Fig. 6 may help to yield some new concept about the optimality model or the design principle of the entire vascular tree (34). In addition to such a large scale problem, Murray's law ($m \approx 3$) still holds for neighboring branches, suggesting that the fractal dimension D and the branch length exponent α are also deliberately selected to maintain the functional properties of vascular trees.

A very interesting optimum model of the vascular system has been presented by West et al. (45), to explain the well established allometric scaling law between basal metabolism or oxygen consumption ($\dot{V}O_2$) and the body weight (W_b,), namely $\dot{V}O_2 \propto W_b^a$, $a = 3/4$ (Ref. 37). Their symmetric model of the arterial tree includes the cross-sectional "area preserving" zone ($m = 2$) in a few proximal branches, within which pulsatile variations of the vessel wall via internal pressure pulsation are prevailing and play an important role in yielding the predicted relationship of $a = 3/4$, instead of $a = 1$ under the steady flow condition. The validity of this model may be certified when some physiological or biomechanical evidence is presented to confirm that the amount of energy dissipation due to pulsations in the major arteries is large enough to explain a shift of the body mass exponent of basal metabolism (a) from 1 in the steady state to 3/4 in the pulsatile state. Zamir (46) suggested that during pulsatile flow at a low-frequency power dissipation due to the oscillatory flow part in the vascular system amounts to about one-half of that required for the steady flow part.

The fractal model in this study can also develop some scope of the scaling problems (37) via the allometric assessment of the terminal numbers in the vascular trees. According to Holt et al. (12), the radius of the aorta (r_o, cm) in mammals is expressed as a function of their body weight (W_b, kg) as follows:

$$r_o = 0.205 W_b^{0.36}$$

By substituting the above into *Eq. 7* with the values of $D + \alpha = 2.88$ and $r_t = 4 \times 10^{-4}$ cm, we obtain the number of terminals (systemic arterioles) N_b (r_t):

$$N_b(r_t) = \left[\frac{4 \times 10^{-4}}{0.205 W_b^{0.36}} \right]^{-2.88} = 6.367 \times 10^7 W_b^{1.04}. \qquad (14)$$

Consequently, the arteriolar number $N_b(r_t)$ in a 70-kg human is estimated to be 5.2×10^9, which is consistent with the estimates for the capillary number in the human systemic vascular beds of approximately $2 \sim 4 \times 10^{10}$ (6, 7), since several capillaries are ordinarily observed to branch off from an arteriole in the vascular bed. Of real importance in *Eq. 14,* however, is the body weight exponent of 1.04, being very close to 1. This implies that the density of terminal arterioles in the body is nearly equal in all mammals, despite large differences in the body weight itself ranging from a few grams to several tons (37). In addition, the relative weight of an organ to total body weight is known to be constant among mammals, with few exceptions (37). It is therefore likely that the density level of terminals in a certain organ is uniform in these animals, although the individual densities may differ from organ to organ. This hypothesis is supported by the fact that, in the lungs of terrestrial mammals, each alveolus is nearly equal in size, whereas the total surface area of alveoli and the capillary volume surrounding them are almost proportional to W_b (the exponents of which are 0.95 and 1.00, respectively Ref. 8). Furthermore, our preceding model analyses of mammalian skeletal muscles (1, 18) demonstrated that the structure of the capillary-tissue arrangement (Krogh's cylinder) is most efficiently tailored for oxygen delivery to tissue during heavy muscular exercise and that the optimum radius of the cylinder is scale-independently constant (the exponent of $W_b = -0.009$). These findings suggest that for any organ, the basic unit composed of a single capillary and some organ-specific cells is uniform in size and shape in mammal species, probably because the unit is designed a priori to attain the maximum efficiency in transcapillary substance exchange during the highest metabolic activity in tissue. The organ size proportional to W_b is mainly ascribed to the accumulated number of the basic units. When these uniform units are compactly arranged in a space and are connected with a vascular system ruled by Murray's law ($m \approx 3$) and with a similarly designed excretory system if necessary, the consequence may bring about a model of the optimum organ, provided with the highest functional efficiency. If the terminal arterioles in an organ are uniformly distributed as discussed above, we can define an infarct index, a quotient of clinical significance. When the flow through an artery of physiological radius r is occluded in an organ, the ratio of the infarct tissue mass to the whole organ, $I(r)$, is written from *Eqs. 7* and *13* as:

$$I(r) = \frac{\left(\frac{r_t}{r}\right)^{-(D+\alpha)}}{\left(\frac{r_t}{r_o}\right)^{-(D+\alpha)}} = \left(\frac{r}{r_o}\right)^m, \qquad (15)$$

where m is the diameter exponent and r_o is the vascular radius at the origin. The value of this quotient, $0 \leq I(r) \leq 1$, may well reflect the severity of tissue damage in the organ following arterial infarction. In a particular case of coronary infarction, the ratio of ischemic myocardium, $I_c(r)$, is estimated from:

$$I_c(r) = \frac{r^m}{(r_{cl})^m + (r_{cr})^m}, \qquad (16)$$

where r_{cl} and r_{cr} are the radii of the left and right coronary arteries at the roots. As the values of m in the coronary artery have been reported, e.g., 2.7, according to Suwa and Takahashi (41), this myocardial infarct index is readily assessable from routine angiographical data. Extensive applicability of this index in clinical medicine is expected.

APPENDIX A

The expectation of branch number N_b (r) by logarithmic sectioning of the r axis. The aggregated branch length ΔL in *Eq. 3* is defined as an integral for a given range of branch radius. Here we attempt to derive the expectation of this length as a discrete function of radius r.

To do so, we need to notice that the probability density of the fractal distribution $\varphi(r)$ is extremely skewed toward the terminals as shown in *Eq. 1* and the variable range of r is so great, e.g., in the vascular system, that r varies from r_o in centimeter order to r_t in micrometer level (Fig. 3). Accordingly, we introduce an alternative variable, $x = -\ln(r/r_o)$: $dx = -dr/r$, $r = r_o e^{-x}$, which allows to divide the entire variable range into n sections of the same width $\Delta x = (x_t - x_o)/n$: $x_t = -\ln(r_t/r_o)$, $x_o = 0$, and to allocate a largely comparable number of branches to every section. Each regional expectation of the aggregated branch length ($\Delta\bar{L}_i$) in such a logarithmic section is obtained by integrating $l_a(r)dr$ over Δx around the midpoint of the ith section, $x_i = (i - 1/2)\Delta x$, $(i = 1,2,\ldots, n)$:

$$\Delta\bar{L}_i = \int_{x_i-\Delta x/2}^{x_i+\Delta x/2} l_a(r)dr = \int_{x_i-\Delta x/2}^{x_i+\Delta x/2} \lambda\kappa r_o^{-D} e^{Dx} dx \approx \lambda\kappa r_i^{-D}\Delta x, \qquad (\because r_i = r_o x_i)$$

if Δx is adequately small. Therefore, the mean aggregated length at each section ($\bar{L}_{ai}$) is given by $\bar{L}_{ai} = \Delta\bar{L}_i/\Delta x = \lambda\kappa r_i^{-D}$. On the other hand, the branch length at the same midpoint (L_{bi}) is expressed from *Eq. 6* as $L_{bi} = \beta x_i^{\alpha}$. Then, the ratio $\bar{L}_{ai}/L_{bi}$ represents the expectation of branch number N_{bi} at the ith section:

$$N_{bi} = \frac{\bar{L}_{ai}}{L_{bi}} = \frac{\lambda\kappa}{\beta} r_i^{-D-\alpha}.$$

The branch number $N_b(r)$ at radius r is obtained from the above, by taking n to infinity ($n \to \infty$) and rewriting $r_i \to r$ and $N_{bi} \to N_b(r)$:

$$N_b(r) = \frac{\lambda\kappa}{\beta} r^{-D-\alpha} = \left(\frac{r}{r_o}\right)^{-D-\alpha},$$

since the branch number at the origin is equal to 1 ($\lambda\kappa/\beta = r_o^{D+\alpha}$). *Equation 7* in the text has been deduced.

APPENDIX B

The total flow and other functional parameters in Eq. 8 in an asymmetric branching system. It is obvious that if the branching system is symmetric, the functional parameters such as cross-sectional area (A_c), mean flow velocity (U_m), individual branch flow (F_b), and wall shear rate ($\dot{\gamma}_w$) can be explicitly expressed by *Eq. 8.* Here we show that this satisfactory condition (the symmetry of branch bifurcations) is not a necessary condition for these parameters, if they represent the mean values (expectations) for the same radius branches.

First we examine that under a steady flow condition, the total flow through branches of an arbitrary radius (r) is equal to that at the origin, F_{bo}, although the branch system includes asymmetric bifurcations. Now, let us consider an ordinary tree, in which the branches ever reduce the radii toward the terminals but discontinuously with no tapering in each branch. If the radius of a mother branch at a branching point is larger than the variable (r) and the radius of either daughter branch becomes equal to or less than r by a single dichotomy, the branching point may be termed a crossing site of the radius level, r. The sum of the fluid flow through the daughter branches, not exceeding r in the radius at every crossing site, may be regarded as the total flow $F(r)$ at radius r. Now, note that any stream line starting from the origin must pass the crossing site of the level r, once and only once, until it reaches the terminals. Then it is obvious that the total flow $F(r)$ at the level r is equal to the flow at the origin, F_{bo}. This means that the total flow $F(r)$ is constant for any r level in the range, $r_t \le r \le r_o$, so long as the fluid does not leak out from the duct wall.

The above argument also indicates that the total flow $F(r)$ at radius r can be determined, regardless of how many branches of asymmetric bifurcation are involved at the crossing sites. It implies that the total flow $F(r)$ is preserved at a constant at any level of r, irrespective of the heterogeneity in the branching architecture. In addition, the expectation of branch number $N_b(r)$ determined in APPENDIX A is not concerned with branch asymmetry. Therefore, the heterogeneity in the branching system has no influence on the functional parameters in *Eq. 8,* because they are all determined by $N_b(r)$ and $F(r)$. It is thus evident that the symmetry of the branching system is not necessarily required to assess the functional parameters in *Eq. 8,* provided that they are regarded as the mean values (expectations) over the same radius branches.

REFERENCES

1. **Baba K, Kawamura T, Shibata M, Sohirad M, Kamiya A.** Capillary-tissue arrangement in the skeletal muscle optimized for oxygen transport in all mammals. *Microvasc Res* 49: 163–179, 1995.
2. **Bassingthwaite JB, Liebovitch LS, West BJ.** *Fractal Physiology.* Oxford: Oxford University Press, 1994.
3. **Dawson CA, Krenz GS, Karau KL, Haworth ST, Hanger CC, Linehan JH.** Structure-function relationships in the pulmonary arterial tree. *J Appl Physiol* 86: 569–583, 1999.
4. **Fåhraeus R, Lindqvist T.** The viscosity of the blood in narrow capillary tubes. *Am J Physiol* 96: 562–568, 1931.
5. **Family F, Masters BR, Platt DE.** Fractal pattern formation in human retinal vessels. *Physica D* 38: 98–103, 1989.
6. **Folkow B, Neil E.** *Circulation.* Oxford: Oxford University Press, 1971.
7. **Fung YC.** *Biomechanics: Circulation* (2nd ed.). New York: Springer-Verlag, 1996.
8. **Gehr P, Mwangi DK, Ammann A, Maloiy GMO, Taylor CR, Weibel ER.** Design of the mammalian respiratory system. V. Scaling morphometric pulmonary diffusing capacity to body mass: wild and domestic mammals. *Resp Physiol* 44: 61–86, 1981.
9. **Gillis HL, Lutchen KR.** How heterogeneous bronchoconstriction affects ventilation distribution in human lungs: a morphometric model. *Ann Biomed Eng* 27: 14–22, 1999.
10. **Glenny RW, Robertson HT, Yamashiro S, Bassingthwaight JB.** Application of fractal analysis to physiology. *J Appl Physiol* 70: 2351–2367, 1991.
11. **Haynes RH.** Physical basis of the dependence of blood viscosity on tube radius. *Am J Physiol* 198: 1193–1200, 1960.
12. **Holt JP, Rhode EA, Holt WW, Kines H.** Geometric similarity of aorta, venae cavae, and certain of their branches in mammals. *Am J Physiol Regul Integr Comp Physiol* 241: R100–R104, 1981.
13. **Horsfield K, Cumming G.** Morphology of the bronchial tree in man. *J Appl Physiol* 24: 373–383, 1968.
14. **Horsfield K, Thurlbeck A.** Relation between diameter and flow in branches of the bronchial tree. *Bull Math Biol* 43: 681–691, 1981.
15. **Kamiya A, Bukhari R, Togawa T.** Adaptive regulation of wall shear stress optimizing vascular tree function. *Bull Math Biol* 46: 127–137, 1984.
16. **Kamiya A, Togawa T.** Optimal branching structure of the vascular tree. *Bull Math Biophys* 34: 431–438, 1972.
17. **Kamiya A, Togawa T.** Adaptive regulation of wall shear stress to flow change in the canine carotid artery. *Am J Physiol Heart Circ Physiol* 239: H14–H21, 1980.
18. **Kamiya A, Wakayama H, Baba K.** Optimality analysis of vascular-tissue system in mammals for oxygen transport. *J Theor Biol* 162, 229–242, 1993.
19. **Karau K, Krenz GS, Dawson CA.** Branching exponent heterogeneity and wall shear stress distribution in vascular trees. *Am J Physiol Heart Cir Physiol* 280: H1256–H1263, 2001.
20. **Kassab GS.** Scaling laws of vascular trees: of form and function. *Am J Physiol Heart Circ Physiol* 290: H894–H903, 2006.
21. **Kitaoka H, Itoh H.** Spatial distribution of the peripheral airways. Application of fractal geometry. *Forma* 6: 181–191, 1991.
22. **Kitaoka H, Suki B.** Branching design of the bronchial tree based on a diameter-flow relationship. *J Appl Physiol* 82: 968–976, 1997.
23. **Majumdar A, Alencar AM, Buldyrev SV, Hantos Z, Lutchen KR, Stanley HE, Suki B.** Relating airway diameter distributions to regular branching asymmetry in the lung. *Phys Rev Lett* 95: 16810-1–168101-4, 2005.
24. **Mandelbrot BB.** *The Fractal Geometry of Nature.* New York: Freeman 1983.
25. **Matsumoto T, Hayashi K.** Mechanical and dimensional adaptation of rat aorta to hypertension. *J Biomech Eng* 116: 278–283, 1994.
26. **Matsuo T, Nakakubo M, Yamamoto K.** Scale invariance of spatial distributions of tree branches, leaves, and petals. *Forma* 12: 91–98, 1997.

27. **Matsuo T, Okeda R, Takahashi M, Funata M.** Characterization of bifurcating structures of blood vessels using fractal dimensions. *Forma* 5: 19–27, 1990.
28. **Morse DR, Lowton JH, Dodson MM, Williamson MH.** Fractal dimension of vegetation and the distribution of arthropod body length. *Nature* 314: 731–733, 1985.
29. **Murray CD.** The physiological principle of minimum work. I. The vascular system and the cost of blood volume. *Proc Natl Acad Sci USA* 12: 207–214, 1926.
30. **Murray CD.** A relationship between circumference and weight in trees and its bearing on branching angles. *J Gen Physiol* 10: 725–729, 1927.
31. **Nelson TR, Manchester DK.** Modeling of lung morphogenesis using fractal geometries. *IEEE Trans Med Imag* 7: 321–327, 1988.
32. **Nicklas KJ.** *Plant Biomechanics.* Chicago: The University of Chicago Press, 1992.
33. **Painter PR, Edén P, Bengtsson HU.** Pulsatile blood flow, shear force, energy dissipation and Murray's law. *Theor Biol Med Model* 3: 31–40, 2006.
34. **Pries AR, Secomb TW, Gaehtgens P.** Design principles of vascular beds. *Circ Res* 77: 1017–1023, 1995.
35. **Rosen R.** *Optimality Principles of Biology.* London: Butterworths, 1967.
36. **Rothe CF.** Venous system: physiology of the capacitance vessels. In: *Handbook of Physiology. The Cardiovascular System. Peripheral Circulation.* Bethesda, MD: Am Physiol Soc 1983, sect. 2, vol. 3, chapt. 13, p. 397–452.
37. **Schmidt-Nielsen K.** *Scaling: Why is Animal Size So Important?* Cambridge: Cambridge University Press, 1984.
38. **Schmidt-Nielsen K.** *Animal Physiology: Adaptation and Environment.* Cambridge: Cambridge University Press, 1997.
39. **Sernetz M, Wübbeke J, Wlczek P.** Three-dimensional image analysis and fractal characterization of kidney arterial vessels. *Physica A* 191: 13–16, 1992.
40. **Shibusawa S.** Modelling the branching growth fractal pattern of the maize root system. *Plant Soil* 165: 339–347, 1994.
41. **Suwa N, Takahashi T.** *Morphological and Morphometrical Analysis of Circulation in Hypertension and Ischemic Kidney.* München, Germany: Urban & Schwarzenberg, 1971.
42. **Tchebichef MP.** L'intégration des différentielles irrationnelles. *Journ de Math* 18: 87–111, 1853.
43. **Weibel ER.** *Morphometry of the Human Lung.* New York: Academic, 1963.
44. **West BJ, Bhargava V, Goldberger AL.** Beyond the principle of similitude: renormalization in the bronchial tree. *J Appl Physiol* 60: 1089–1097, 1986.
45. **West GB, Brown JH, Enquist BJ.** A general model for the origin of allometric scaling laws in biology. *Science* 276: 122–126, 1997.
46. **Zamir M.** *The Physics of Pulsatile Flow.* New York: Springer-Verlag, 2000.
47. **Zweifach BW, Lipowsky HH.** Pressure-flow relations in blood and lymph microcirculation. In: *Handbook of Physiology. The Cardiovascular System, Microcirculation.* Bethesda, MD: Am. Physiol. Soc, 1984, sect. 2, vol. 4, chapt. 7, p. 251–307.